

Two rare $\{M_2(MoO_4)_2\}_n$ chain-contained molybdate-based metal-organic complexes with bis-pyrazole-bis-amide ligand: fluorescent sensing and photocatalysis performance

Xiuli Wang^{*#}, Xiang Pan[#], Xiang Wang*, Yan Li and Guocheng Liu

**Corresponding authors, E-mail addresses: wangxiuli@bhu.edu.cn (X. L. Wang); E-mail: wx_2007@163.com (X. Wang).*

College of Chemistry and Chemical Engineering, Professional Technology Innovation Center of Liaoning Province for Conversion Materials of Solar Cell, Bohai University, Jinzhou 121013, P. R. China.

#Theses authors contributed equally to this work.

Supporting Information

Table S1. Selected bond distances (\AA) and angles ($^\circ$) for complexes **1–2**.

Complex 1			
Co(1)–O(3)	2.054(4)	Co(1)–N(1)	2.111(4)
Co(1)–O(4)#1	2.079(4)	Co(1)–N(2)	2.128(4)
Co(1)–O(5)#2	2.089(4)	Co(1)–O(1)	2.184(3)
O(3)–Co(1)–O(4)#1	93.54(15)	O(5)#2–Co(1)–N(2)	93.14(15)
O(3)–Co(1)–O(5)#2	88.75(14)	N(1)–Co(1)–N(2)	162.09(18)
O(4)#1–Co(1)–O(5)#2	177.69(14)	O(3)–Co(1)–O(1)	178.09(15)
O(3)–Co(1)–N(1)	93.67(16)	O(4)#1–Co(1)–O(1)	88.16(14)
O(4)#1–Co(1)–N(1)	88.49(16)	O(5)#2–Co(1)–O(1)	89.54(14)
O(5)#2–Co(1)–N(1)	91.65(16)	N(1)–Co(1)–O(1)	87.24(16)
O(3)–Co(1)–N(2)	103.68(16)	N(2)–Co(1)–O(1)	75.55(15)
O(4)#1–Co(1)–N(2)	86.04(16)		

Symmetry code for **1**: #1 –x + 1/2, y + 1/2, –z + 3/2; #2 –x + 1/2, y – 1/2, –z + 3/2

Complex 2			
Zn(1)–O(4)#1	2.014(3)	Zn(1)–N(1)	2.124(3)
Zn(1)–N(2)	2.093(3)	Zn(1)–O(2)	2.146(3)
Zn(1)–O(5)#2	2.120(3)	Zn(1)–O(1)	2.299(3)
O(4)#1–Zn(1)–N(2)	97.17(12)	O(5)#2–Zn(1)–O(2)	174.51(10)
O(4)#1–Zn(1)–O(5)#2	90.37(11)	N(1)–Zn(1)–O(2)	85.21(12)
N(2)–Zn(1)–O(5)#2	92.40(12)	O(4)#1–Zn(1)–O(1)	178.03(11)
O(4)#1–Zn(1)–N(1)	105.43(12)	N(2)–Zn(1)–O(1)	84.13(11)
N(2)–Zn(1)–N(1)	156.71(13)	O(5)#2–Zn(1)–O(1)	88.10(10)
O(5)#2–Zn(1)–N(1)	92.98(12)	N(1)–Zn(1)–O(1)	73.42(11)
O(4)#1–Zn(1)–O(2)	95.10(11)	O(2)–Zn(1)–O(1)	86.42(11)
N(2)–Zn(1)–O(2)	87.29(12)		

Symmetry code for **2**: #1 –x + 3/2, y – 1/2, –z + 3/2; #2 x, y – 1, z

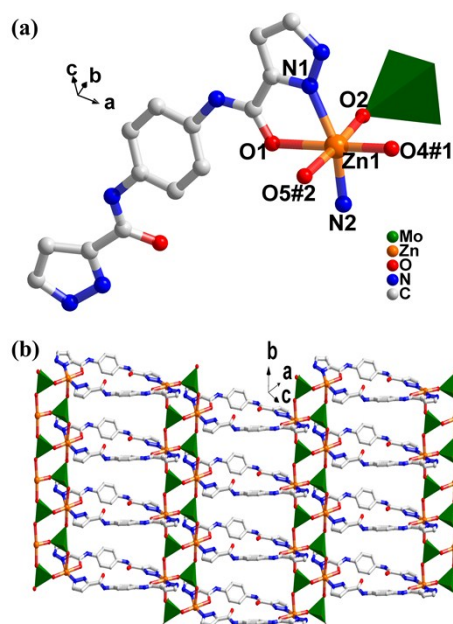


Figure S1. (a) Ball/stick/polyhedron view of the asymmetric unit of complex **2**. The hydrogen atoms are omitted for clarity; (b) The 2D structure of complex **2**.

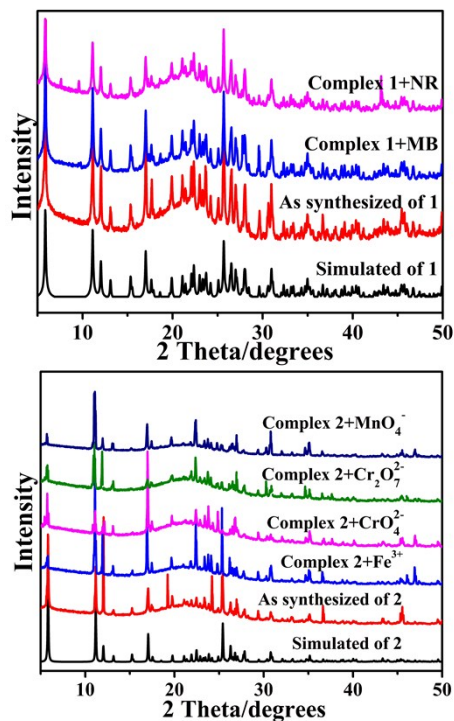


Figure S2. PXRD patterns of complexes **1–2**.

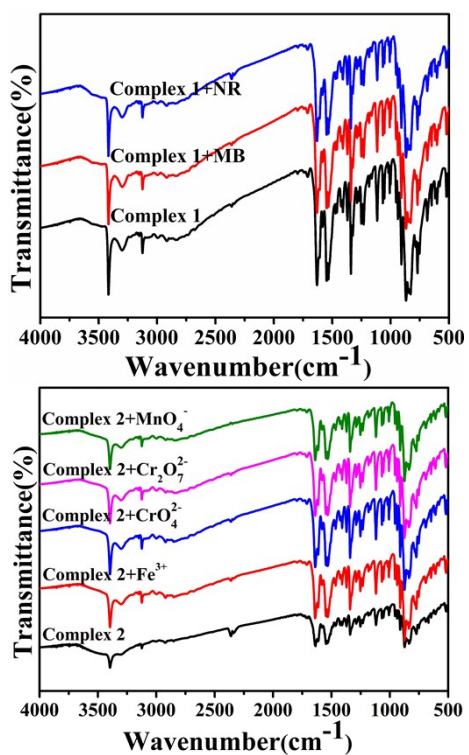


Figure S3. The IR spectra of complexes **1–2**.

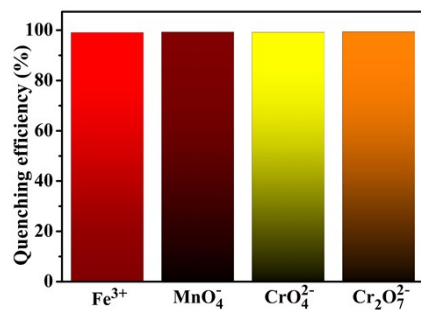


Figure S4. Fluorescence quenching efficiency of complex **2**.

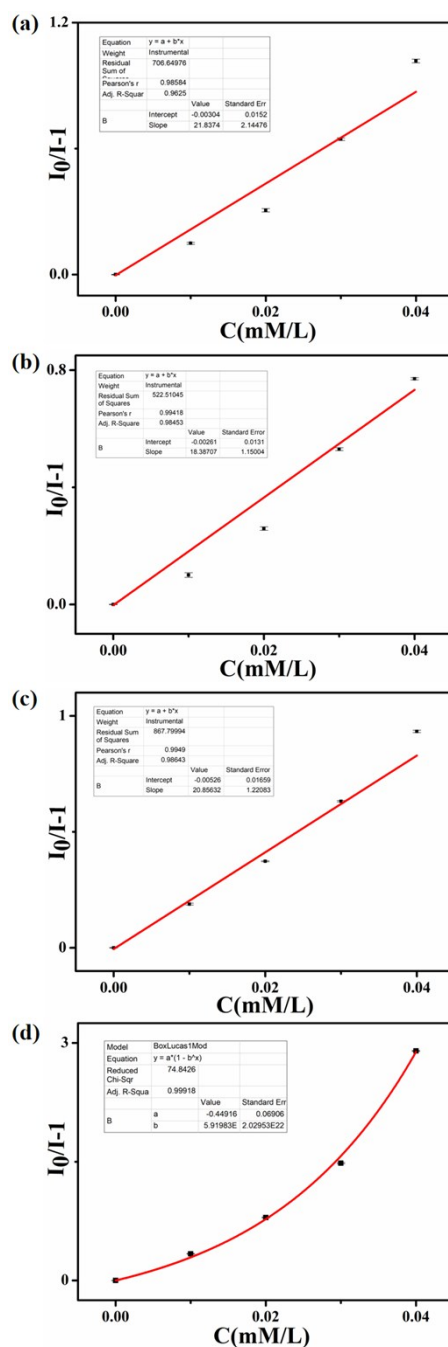


Figure S5. (a) The fluorescence intensity *vs.* Fe^{3+} , (b) MnO_4^- , (c) CrO_4^{2-} and (d) $\text{Cr}_2\text{O}_7^{2-}$ concentration plot.

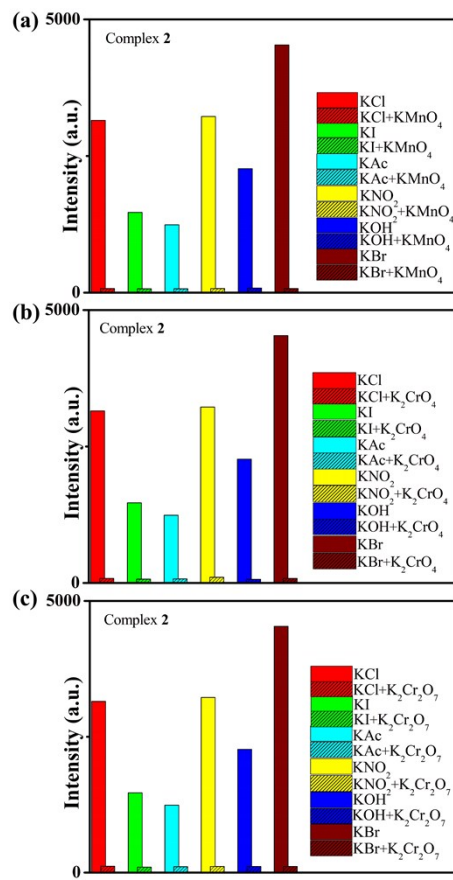


Figure S6. Fluorescence emission intensities of **2** at room temperature upon the addition of MnO_4^- (a), CrO_4^{2-} (b) and $\text{Cr}_2\text{O}_7^{2-}$ (c) anions.

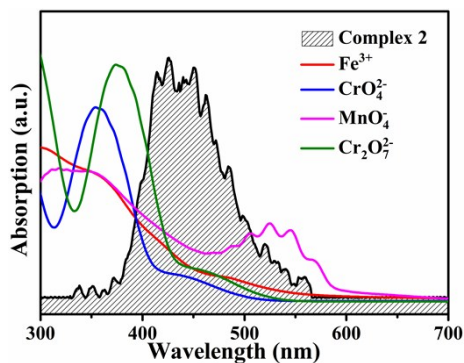


Figure S7. UV-Vis absorption spectra of Fe^{3+} , MnO_4^- , CrO_4^{2-} and $\text{Cr}_2\text{O}_7^{2-}$ aqueous solution.

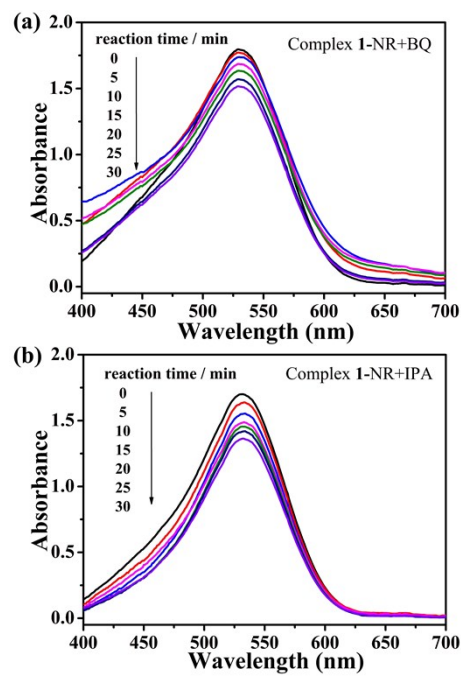


Figure S8. Trapping experiments of active species (a) BQ and (b) IPA during the photocatalytic degradation NR reaction for complex **1**.